The Hubble Deep Field

Henry C. Ferguson
Space Telescope Science Institute, Baltimore, MD 21218
ferguson@stsci.edu

Abstract

We review progress in analysis and interpretation of the Hubble Deep Field (HDF) images and supporting observations. The availability of data at a wide range of wavelengths, and spectroscopic redshifts for a large number of galaxies, provides the most comprehensive picture of the field galaxy population at magnitudes fainter than $I = 25$. The HDF images themselves reveal large numbers of irregular and peculiar galaxies, which constitute an increasing fraction of the galaxy population toward faint magnitudes, making up roughly half of the total number of galaxies by $I \sim 25$. The trend toward irregular morphologies is also reflected in the colors, which for the majority of galaxies are as blue as local star-forming irregular galaxies. Redshift surveys are now approaching completion to limits $I \sim 23$; even at this limit the median redshift is below $z = 0.7$. However, a small number of galaxies at $z > 2$ reveal themselves through their colors and many are confirmed spectroscopically. The density of these high-redshift galaxies is lower than expected from models where elliptical galaxies and spiral galaxy bulges form in rapid star-formation episodes at high redshift. If such models are to survive, a large luminous population of galaxies must be hidden by dust or observational selection effects. Barring such large corrections, the HDF data, combined with other surveys, suggests a peak in the global metal enrichment rate at $1 \lesssim z \lesssim 2$. The integrated flux from galaxies is dominated by objects within the limits of spectroscopic surveys. Fainter objects in the HDF appear largely to be at redshifts $z < 2$, but their number densities are higher than expected from pure-luminosity evolution models, and their relation to local galaxy populations is still unclear.

1 Introduction

Among the most striking images returned by the Hubble Space Telescope is the view of distant galaxies recorded during 10 straight days of observation in December 1995. These images cover an area of sky about 2.6 arcminutes on a side, which is roughly the angular size of the period at the end of this sentence viewed from reading distance. The faintest sources in the image have V magnitudes of about 30, equivalent to one photon per week striking the human eye. The Hubble Deep Field (HDF) image reveals galaxies about 15 times fainter than can be seen in the deepest images taken from the ground. The image provides both a new source of inspiration for those interested in the wonders of the universe, and the latest and

greatest source of data in a long line of surveys that push the limits of technology to attempt to see what galaxies like our own looked like in their early stages of evolution.

1.1 Motivation and Background

> *If we knew what it was we were doing, it would not be called research, would it? (Albert Einstein)*

There were a number of reasons why, in the beginning of 1995, it seemed sensible to contemplate a project like the HDF. After the successful mission to refurbish the initially flawed HST optics, in December 1993, efforts to resolve and study distant galaxies became a high priority. Among the first images returned after the refurbishment were Dressler's beautiful images of CL 0939+4713, and Dickinson's impressively deep images of the cluster around radio galaxy 3C324 (Dressler et al. 1994; Dickinson 1995a). These and other images made it clear that HST would be a useful engine for studying distant galaxies. This was not entirely obvious beforehand. Prior to launch, simulations based on fairly conservative assumptions suggested that HST would not provide an overwhelming advantage over ground-based telescopes for studies of distant galaxies (Bahcall, Guhathakurta, & Schneider 1990):

> *Our results show that the most sensitive exposures achieved so far from the ground reveal more galaxies per unit area than will be seen by planned HST observations unless galaxy sizes decrease with the maximum rate consistent with ground-based observations. In this, the most favorable case for HST, the space exposures will show almost as many galaxy images as have been observed so far in the most sensitive ground-based data.*

It was apparent from the images returned in 1994 that this prediction was far too pessimistic. The unexpectedly small angular sizes of faint galaxies gave HST a great advantage in detection over ground-based instruments. For well-resolved galaxies, HST observations opened the window to studies of galaxy morphology and structure, which had been exceedingly difficult beyond $V \sim 20$ from the ground. Results on the evolution of galaxy scale lengths and morphologies, on the evolution of clustering and the galaxy merger rate, and on the presence of unusual types of galaxies (e.g. chains) began to appear in conferences and in the literature (Mutz et al. 1994; Schade et al. 1995; Cowie, Hu, & Songaila 1995; Griffiths et al. 1996).

In this context, the idea of using HST to do a deep field survey began to look quite attractive, and was eventually adopted as the prime use of Director's discretionary time for the fifth HST observing cycle.

1.2 The effects of geometry

Historically, the motivation for deep surveys has been to test cosmological models. Such tests were among the defining goals of the 5-m Hale telescope and the Hubble

Space Telescope. The goal of measuring the geometry of the universe has eluded us due to the difficulty of disentangling the effects of galaxy selection and evolution from the effects of cosmic geometry. Nevertheless, it is worth noting that the effects of geometry are not subtle for galaxies at the distances now being probed by HST. Even if it seems beyond hope to deduce the geometry of the universe from galaxy surveys, we cannot ignore it in trying to decipher galaxy evolution.

Carroll, Press, & Turner (1992) present a useful outline of geometric effects relevant to deep surveys. The contributions of matter and the cosmological constant to the expansion of the universe at the current epoch are parametrized by

$$\Omega_M \equiv \frac{8\pi G}{3H_0^2}\rho_{M0} \quad \Omega_\Lambda \equiv \frac{\Lambda}{3H_0^2} \quad , \tag{1}$$

where ρ_M is the density of matter, and the subscript 0 refers to the current epoch. For the "flat" universe preferred by most inflationary models, $\Omega_M + \Omega_\Lambda = 1$. In general $\Omega_M + \Omega_\Lambda = \Omega_{\rm tot}$, which can be either less than or greater than 1. For computing the ages, angular sizes, and apparent brightnesses of galaxies, it is useful to define a quantity $A(z)$, such that

$$A(z) \equiv [(1+z)^2(1+z\Omega_M) - z(2+z)\Omega_\Lambda]^{-1/2}. \tag{2}$$

The lookback time to an object at redshift z_1 is then given by

$$t_{LB}(z_1) = H_0^{-1}\int_0^{z_1}(1+z)^{-1}A(z)dz. \tag{3}$$

The flux received from a galaxy of luminosity L is

$$f = L/4\pi d_L, \tag{4}$$

where the luminosity distance d_L is given by

$$d_L(z_1) = \frac{c}{H_0}(1+z)\int_0^{z_1} A(z)dz, \tag{5}$$

for a flat universe with $\Omega_{\rm tot} = 1$.

Even prior to the discovery of normal star-forming galaxies at $z \approx 3$ (Steidel et al. 1996b) it was clear that HST should be capable *in principle* of detecting galaxies at high redshift. The present-day luminosity function of galaxies is reasonably well approximated by the combination of a power-law and an exponential function (Schechter 1976):

$$\phi(L)dL = \phi^*(\frac{L}{L^*})^\alpha e^{-(L/L^*)}\frac{dL}{L^*} \tag{6}$$

Locally, the density of L^* galaxies, at the characteristic "knee" of this function, is about $0.002{\rm Mpc}^{-3}\,{\rm mag}^{-1}$, for $H_0 = 50{\rm kms}^{-1}{\rm Mpc}^{-1}$ (Loveday et al. 1992; Lin et al. 1996). These densities translate into dozens of high-redshift galaxies in the HST field of view. The last column of Table 1 shows the surface densities corresponding to this volume density in intervals $\Delta z = 1$ centered on $z = 2$ and $z = 4$. The HST

Wide Field Planetary Camera 2 (WFPC2) field of view is $1.5 \times 10^{-3}\mathrm{deg}^{-2}$, so the numbers shown correspond to roughly the number of L^* galaxies one might expect to find in the HDF in those redshift intervals, in the absence of evolution. Table 1 also shows the apparent AB magnitude (Oke 1974) that would correspond to an L^* galaxy with a flat spectrum in f_ν, and the age of the universe at redshifts 2 and 4. [1] These comparisons illustrate the huge differences one might expect in the numbers, brightnesses, and ages of distant galaxies purely from geometrical effects.

Table 1. The effects of geometry

Ω_M	Ω_Λ	Ω_{tot}	z	Age of the universe (Gyr)	Apparent mag. of $M = -21.1$ flat spectrum galaxy	Surface density corresponding to $2 \times 10^{-3}\mathrm{Mpc}^{-3}$ $(10^{-3}\mathrm{deg}^{-2})$
0.1	0.0	0.1	2	4.9	25.6	62
			4	2.6	27.9	178
1.0	0.0	1.0	2	2.5	24.8	16
			4	1.2	26.5	30
0.1	0.9	1.0	2	7.5	26.1	160
			4	3.6	28.1	378

1.3 Faint blue galaxies

The classical geometrical tests involve computing the number–magnitude relation $N(m)$, number–redshift relation $N(z)$, and other quantities for an adopted cosmological model and comparing to the observed relations for galaxies (Sandage 1961). Rapid observational progress in the last two decades has improved the data to the point where the statistical uncertainties are small. However, these observations have also revealed that the problem is considerably more complex than originally appreciated.

The complexity of the problem can be illustrated by considering the following measurements of the statistical properties of faint galaxies, available at the time the HDF was being planned.

- *Galaxy counts from the ultraviolet to the infrared.* At blue wavelengths, the $N(m)$ relation is still rising steeply at the limits of ground-based observations, exceeding by a factor of ten the surface density expected for a $q_0 = 0.5$ non-evolving universe. In the K band the counts are flatter and more consistent with mild evolution and $q_0 = 0.5$ (Tyson 1988; Smail et al. 1995; Metcalfe et al. 1995).
- *Galaxy redshift distributions.* Broadly speaking, the observed distributions are unimodal with a median redshift consistent with no-evolution models.

[1] Most magnitudes in this paper are expressed in the *AB* system (Oke 1974), where $m = -2.5 \log f_\nu - 48.60$.

Galaxies at $z < 0.1$ or $z \succ 3$ constitute less than 20% of the counts to $B < 24, I < 22.5$ (Colless et al. 1993; Glazebrook et al. 1995a; Lilly et al. 1995a; Cowie et al. 1996).

- *The amplitude of the angular correlation function.* The faintest galaxies appear to be very weakly clustered to ground-based limits (Efstathiou et al. 1991; Roche et al. 1993; Neuschaefer & Windhorst 1995; Brainerd, Smail, & Mould 1995; Roche et al. 1996).
- *The space density of luminous galaxies at* $z \sim 1$. The K-band luminosity function of absorption-line selected galaxies at these moderate redshifts appears consistent with the bright end of the local luminosity function (Steidel, Dickinson, & Persson 1994). The luminosity function of galaxies with colors redder than Sbc appears to evolve slowly or not at all at to $z \sim 0.7$ (Lilly et al. 1995b).
- *The angular size distribution of faint galaxies* (Im et al. 1995). At $V = 28$ the typical galaxy half-light radius is less than 0.2 arcsec, significantly smaller than expected if the population is dominated by non-evolving L^* galaxies, even for low values of q_0.

Clearly there are other measurable quantities as well, but these five reveal the crux of the problem. Galaxy counts in the B band require a higher surface density of galaxies than expected purely from geometry, especially for $\Omega_M = 1$. The "excess" population is evidently not at extremely high redshift, is made up of reasonably compact galaxies, and is weakly clustered. It was hoped that the combination of high-quality HST data and deep ground-based redshift surveys could help reveal the physical nature of faint blue galaxies.

1.4 Where are the baryons?

One of the more speculative issues that could be addressed with deep images of a more-or-less random patch of sky is whether there are sites of star formation in the early universe that do not correspond to known stellar populations in the local universe. The local "baryon budget" indicates that there is plenty of room for stars to have formed without violating the constraints of primordial nucleosynthesis. Measurements of the helium abundance in low-metallicity dwarf galaxies (Skillman et al. 1994) and the deuterium abundance in metal-poor quasar absorption line systems Tytler, Fan, & Burles (1996) suggest that, for $H_0 = 50$ km s^{-1} Mpc^{-1}, $\Omega_b \approx 0.04$. The total baryonic contribution from galaxies and the known X-ray gas in clusters (Persic & Salucci 1992; Fukugita, Hogan, & Peebles 1997) amounts to $\Omega_b \approx 0.02$. It is thus not inconceivable that a population of stars formed out of these baryons at high redshift, and subsequently faded from view. Remnants of these populations could be hiding, for example, as MACHOs in galactic halos (Alcock et al. 1997), or as a population of extremely low-surface brightness galaxies (Babul & Ferguson 1996). Deep imaging surveys such as the HDF provide a way to search for such sites of star formation.

2 The Hubble Deep Field Observations

The Hubble Deep Field is a carfully selected "random" patch of sky situated in the HST northern continuous viewing zone (CVZ). When the HST orbit pole is favorably aligned, targets in the CVZ can be observed without interference by earth occultations, thus nearly doubling the observing efficiency. This gain in observing efficiency outweighed the advantages of choosing a previously studied field. The properties of the HDF are shown in Table 2.

Table 2. Characteristics of the Hubble Deep Field

Location:	$12^h36^m49.4^s$ $+62°12'58''$
	(Epoch J2000 / WFPC-2 'WFALL FIX' position)
	V3 Position angle = 112°
$E(B-V)$:	0.00
HI column density:	$1.7 \times 10^{20}\mathrm{cm}^{-2}$
DIRBE flux:	< 0.14 MJy/ster
Radio sources:	none with flux > 1 mJy at 3.6 cm
IRAS cirrus:	Local minimum in 100μm maps
Bright stars:	None near the field
Galaxy clusters:	Nearest is 48 armin away

The HDF data were obtained in late December 1995. Roughly 300 individual exposures were combined into the final HDF images. Ten additional short F814W band exposures were taken of adjacent "flanking" fields to aid in source identification for followup observations. The exposures of the central field were registered and resampled onto a grid of $0.04''$ pixels. (They physical WFPC2 detector pixels span 0.1" in the three WF camera channels and 0.045" in the PC channel.) The resampling was done using variable-pixel linear reconstruction (also known as "drizzling") which simultaneously corrects for the WFPC2 geometric distortion and improves the resolution (Fruchter & Hook 1997).

2.1 Filter selection

The selection of filters for the HDF observations represents a balance between the desire for depth and the desire for color information, and practical considerations involving scattered earth light. The final HDF images reach 5σ limiting AB magnitudes of roughly 27.7, 28.6, 29.0, and 28.4 (for an aperture area of 0.2 square arcsec) in the F300W, F450W, F606W, and F814W bandpasses (the number corresponds to the central wavelength in nm), respectively (Williams et al. 1996). The F300W filter was chosen in part because of its utility for identifying galaxies at redshifts $z > 2$ and in part because it could make efficient use of the "bright time" in the orbit.

3 HDF Phenomenology

Since release, the HDF images have been analyzed and interpreted by a large number of different groups for a wide variety of purposes. Among the first analyses were those aimed at cataloging and characterizing the sources present in the images. Table 3 gives a rough indication of the different types of sources and the different kinds of data available.

Table 3. HDF Census and Types of Data

< 20	Stars to $I = 26.3$
~ 3000	Galaxies measured in $U_{300}, B_{450}, V_{606}$, and I_{814}.
~ 300	Galaxies measured in J, H, and K.
~ 130	Measured redshifts (many more in the flanking fields).
~ 26	Galaxies with spectroscopic $z > 2$
$\sim 7 - 14$	ISO detections (6.7 μm and/or 15 μm) (Goldschmidt et al. 1997)
~ 7	6.7 GHz Radio sources (Fomalont et al 1997)
0	sources at 2.8 mm (Wilner et al. 1997)

3.1 Stars

Although it covers only a small area of sky, the depth and color information of the HDF offers a unique probe of the stellar mass function of the Galactic disk and halo. For example, at the 10σ level, an M dwarf with a mass $0.1\,M_\odot$ could be detected in the HDF out to a distance of ~ 2.5 kpc, while a $0.3\,M_\odot$ dwarf would be visible out to 16 kpc. Near its limiting magnitude, the HDF provides another advantage: the contribution from Galactic red giants and supergiants is virtually non-existent. At $I = 26$ a red giant would have to be at a distance of one Mpc to masquerade as a red dwarf. The work on star counts in the HDF builds on similar efforts in other HST images (Bahcall et al. 1994), and confirms these earlier indications that the stellar luminosity function turns over at $M_V \approx -12$ (Flynn, Gould, & Bahcall 1996; Elson, Santiago, & Gilmore 1996; Mendez et al. 1996; Reid et al. 1996; Gould, Bahcall, & Flynn 1997; Kerins 1997; Chabrier & Mera 1997). Hydrogen-burning stars with masses less than $0.3\,M_\odot$ account for less than 1% of the total mass of the Galactic halo. In addition to the nine or so candidate red dwarfs, to a limiting magnitude of $I = 28$ the HDF has about 50 unresolved objects with relatively blue colors. While in principle these could be white dwarfs, this possibility appears to be unlikely as the lack of brighter point sources with similar colors would require that they be located in a shell about the galaxy. More likely, these are unresolved star-forming galaxies.

The HDF results contribute in a small way to the constraints on the initial mass function (IMF) at low masses. Gould, Bahcall, & Flynn (1996) suggest that the HST data on field stars can be reasonably fit with a log-normal IMF of the form

$$\log(\phi) \propto -1.33\log(M/M_\odot) - 1.82[\log(M/M_\odot)]^2. \quad (7)$$

The functional form is the same as that proposed by Miller & Scalo (1979), but the coefficients are different. Recent theoretical arguments in favor of a log-normal IMF have been set out by Adams & Fatuzzo (1996) and Padoan, Nordlund, & Jones (1997). To put the HST results in a larger context, we show in Fig. 1 a compilation of the derived initial mass functions from several different studies, combined with several different functional forms for the IMF that have been proposed in the literature. (The HDF data themselves contribute only to a few points at the low mass end.) The observational data are taken at face value from the papers; no attempt has been made to reconcile the different corrections the authors have applied to go from the LF to the IMF. In practice, the derivation of the IMF from observations of the luminosity function (LF) is complicated by uncertainties in the mass–luminosity relation, and the various corrections that need to be applied for metallicity, age, and binaries. The most robust conclusion that can be drawn is that the IMF is flatter than the Salpeter power-law ($\xi(M) \propto m^{-2.35}$) at low masses.

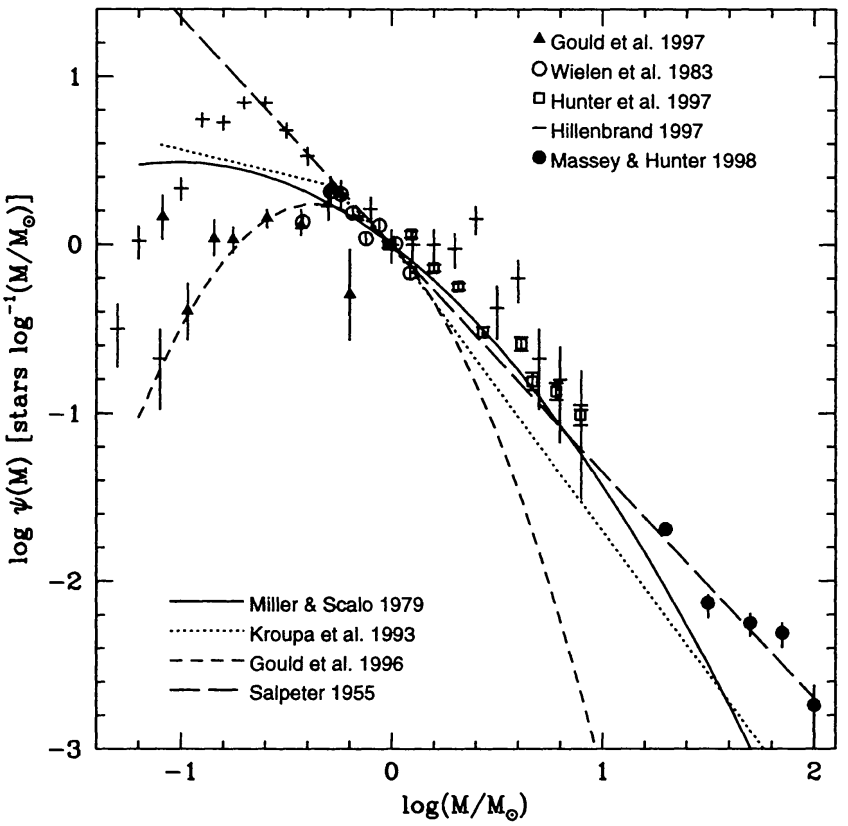

FIG. 1 — The stellar IMF from HST and ground-based observations. The data are for field stars and selected clusters in the Galaxy and the LMC from various ground-based and HST studies. The different measured IMFs have been normalized to $\log(\phi) = 0$ at 1 $M_\odot$. Functional forms proposed in the literature are also shown. The Kroupa et al. (1993) IMF contains a correction for binaries. The various data sets shown have not been corrected for binaries.

3.2 Galaxy Morphologies and Colors

Attempts to extend galaxy classification and quantitative surface photometry to magnitudes fainter than $V \sim 20$ were pioneered by the Medium Deep Survey team (Casertano et al. 1995; Driver et al. 1995; Glazebrook et al. 1995b). By the time of the HDF observations it was clear from such analysis that the galaxy population at $I \sim 23$ contained a larger fraction of irregular or peculiar galaxies than would be expected from a simple extrapolation of galaxy populations in the local universe. However, measurements at fainter magnitudes were hindered by the low signal-to-noise ratio of the MDS data. Several hundred resolution elements above $S/N = 5$ are needed in a galaxy image to make a reasonable attempt at morphological classification or fitting the surface brightness profile. The HDF, with its higher S/N and spatial resolution, presented an opportunity to extend these studies to fainter magnitudes.

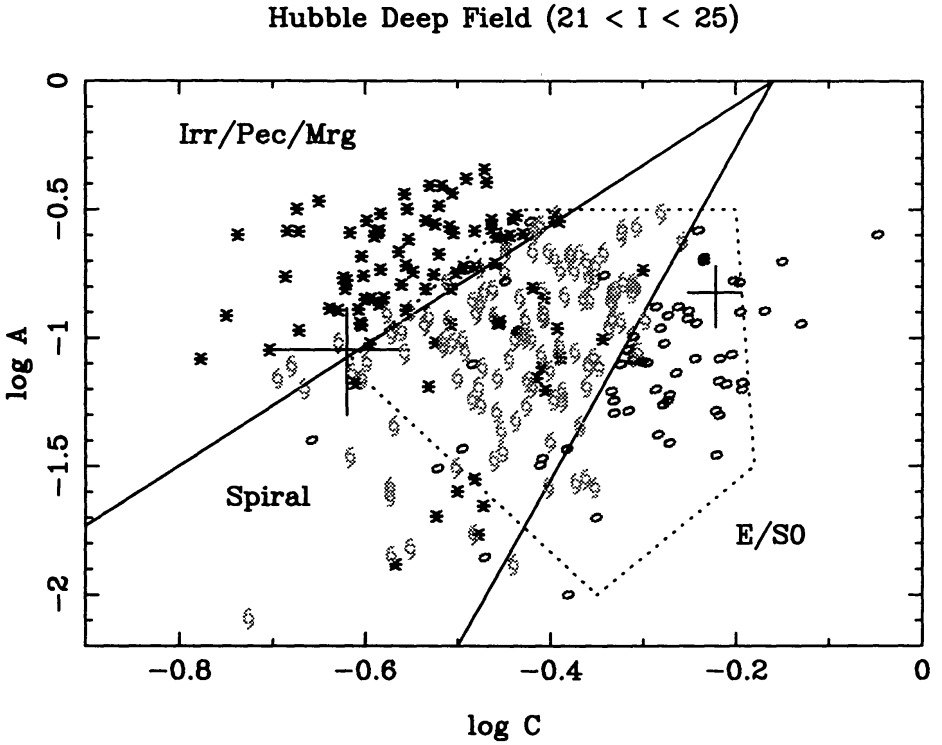

FIG. 2 — Distribution of galaxy morphologies of the brightest 521 galaxies in the Hubble Deep Field. The axes denote measurements of the central concentration and the asymmetry of each galaxy's light profile, while the symbols show the galaxies that were visually classified as spirals, ellipticals, or irregular/peculiar galaxies. The sectors subdivide the diagram into regions where each of these morphological types dominates. Representative error bars in the measured photometric parameters are shown as crosses. The dotted polygon outlines the region populated at similar luminosities in the local universe. From Abraham et al. (1996).

Abraham et al. (1996) used the HDF to extend the MDS results to $I = 25$. They measured the concentration and asymmetry of the galaxy images, and also classified each galaxy by eye. Their basic result is shown in Fig. 2. Both the

photometric parameters and the eyeball classifications indicate that a large fraction of the HDF galaxies have irregular morphologies. Some are reminiscent of local Magellanic irregulars; others are more likely signs of interactions or mergers. The various tests in the Abraham et al. paper and since then (Abraham 1997) have shown that this progression toward later types at high redshifts is not primarily due to resolution, or to the progressive shifting of the I band toward restframe UV wavelengths for higher redshift galaxies. There is a physical change in the mix of galaxies at moderate redshifts $0.5 < z < 1.5$; normal present-day elliptical and spiral galaxies appear to be present in roughly the numbers expected from modest evolution of the present-day luminosity function (or if anything with co-moving densities declining with increasing z; Kauffmann, Charlot, & White 1996). The increase in the space density of galaxies appears due largely to irregular and peculiar galaxies.

Figure 3 shows a color–magnitude diagram in $B_{450} - I_{814}$ for HDF galaxies. For comparison, also shown are the colors for template non-evolving galaxies of different types. The templates for E, Sbc, and Im galaxies are taken from Coleman, Wu, & Weedman (1980), with the extrapolations adopted by Ferguson & McGaugh (1995). The E and Sbc spectra have absolute magnitudes in the F450W band of $B_{450} = -21.1$, roughly L^* for $H_0 = 50\,\mathrm{km\,s^{-1}Mpc^{-1}}$. The Im spectrum is normalized to an absolute magnitude $B_{450} = -18$, more typical of a Magellanic irregular. While the elliptical galaxy template encloses the red envelope of the data reasonably well, there is a large population of galaxies at faint magnitudes that are bluer than the irregular galaxy template at any redshift. Also, there is a substantial population of galaxies with colors suggestive of redshifts $z > 2$.

3.3 Galaxy Sizes

The size evolution of normal luminous spiral galaxies has been studied by several groups, mostly using data from surveys other than the HDF. Roche et al. (1998) fit exponentials and deVaucouleurs profiles to the images of galaxies in the MDS database and the HDF. Most of the galaxies in their sample have measured redshifts, although they consider color-selected high-redshift galaxies from the HDF as well. They find no evidence for evolution in the rest-frame sizes or surface brightnesses of normal spirals and ellipticals out to z=0.35. Among disk galaxies at higher redshift they find evidence for strong evolution, with central surface brightnesses increasing by about 1 magnitude between $z = 3$ and $z = 0.8$ (see also Schade et al. 1995). Lilly et al. (1998), using images of galaxies in the Canada-France Redshift Survey (CFRS) and the Low Dispersion Spectroscopic Survey (LDSS), find no evidence for size evolution of large (exponential scale length $\alpha > 3.2\,h_{50}^{-1}\,\mathrm{kpc}$) galaxies out to $z \sim 1$. They also see no evidence for evolution in the co-moving densities of large disk galaxies. However, the average rest-frame B-band extrapolated central surface brightness brightens by about 0.8 mag out to $z = 0.7$. The results of these studies are broadly consistent with a picture in which large spiral galaxies form gradually, with slowly decreasing star-formation rates per unit area.

The elliptical galaxies in the HDF have been studied by Fasano et al. (1998).

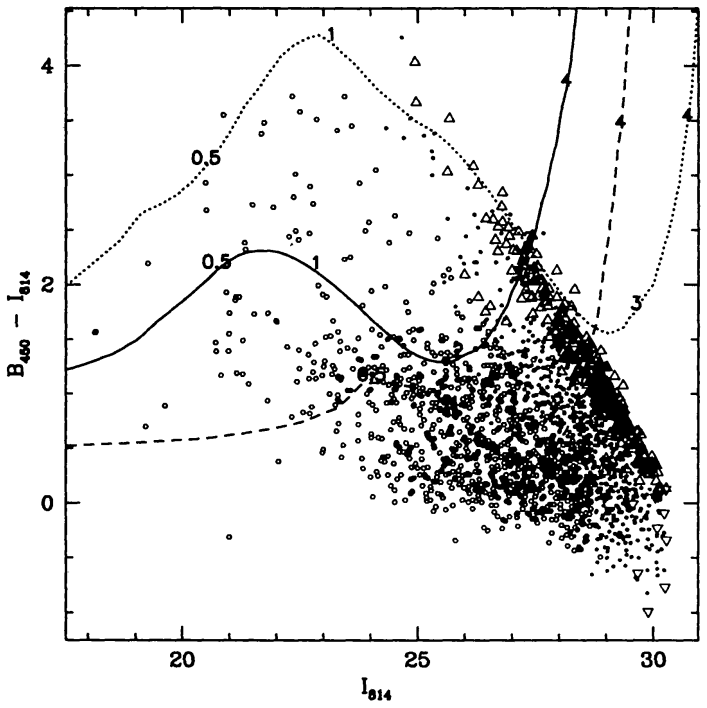

FIG. 3 — Color-magnitude diagram $B_{450} - I_{814}$. Galaxies detected at more than 5σ are shown as large hexagons. Galaxies detected at less than 5σ are smaller hexagons. Galaxies either undetected in F450W or detected at less than 2σ significance are shown as open triangles at the position of the 2σ limit on the color. Also shown are the colors of fiducial non-evolving spectra of E, Sbc, and Im galaxies (see text), as dotted, solid, and dashed curves, respectively, with redshift indicated by the labels. From Williams et al. (1996).

They compare the size-luminosity relation for 48 objects (23 with spectroscopic redshifts) to the Kormendy (1985) relation for local ellipticals. A significant offset between the local and the distant samples is seen, but can be accounted for entirely by $(1+z)^4$ cosmological dimming, k-corrections, and corrections for passive evolution from the models of Bressan, Chiosi, & Fagotto (1994). At redshifts $z \approx 2-3$ they note a statistically significant lack of large ellipticals.

At magnitudes fainter than $I = 25$ morphological classification and profile fitting become quite difficult. Ferguson (1998) studied the distribution of first-moment radii and modeled the selection boundaries of the HDF in size and magnitude. The surface-brightness selection effects are severe enough that a normal, non-evolving L^* spiral galaxy would disappear from view at $z \sim 1.2$ at $I_{814} \sim 25.5$ even though the nominal magnitude limit of the HDF is more than three magnitudes fainter. Still, even at magnitudes $I_{814} \approx 25$ where L^* spirals could be seen, the HDF galaxy counts are clearly dominated by objects more compact than L^* spirals. Fainter than $I_{814} = 27.5$ the locus of HDF galaxy sizes is tightly constrained by selection, and there is very little information on the *intrinsic* size distribution of the objects.

3.4 Spectroscopic and Photometric Redshifts

Spectroscopic followup of the HDF has been carried out mostly from the W. M. Keck Obsevatory on Mauna Kea, by a variety of different groups (Cohen et al. 1996; Hogg et al. 1998; Steidel et al. 1996a; Zepf, Moustakas, & Davis 1997; Lowenthal et al. 1996; Phillips et al. 1996; Guzman et al. 1996; Dickinson 1998a). Strategies vary, with some groups aiming for magnitude limited samples, others targeting high-redshift objects, and others targeting interesting compact or potentially lensed objects. The end result is a heterogeneous set of about 130 redshifts in the central field. The redshift distribution as of early 1998 is shown in Fig. 4.

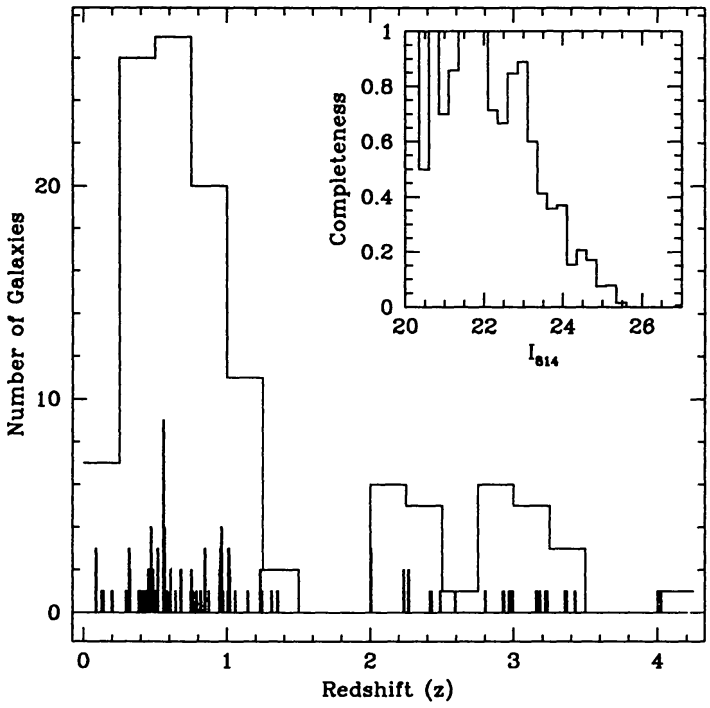

FIG. 4 — Spectroscopic redshifts in the Hubble Deep Field, as of early 1998. The main panel shows the redshift distribution in bins of $\Delta z = 0.5$ and in bins of $\Delta z = 0.005$. The finely-binned histogram illustrates the pronounced clumpiness of the redshift distribution, with many galaxies inhabiting structures less than 20 co-moving Mpc across. The inset shows the fraction of galaxies in the central field that have measured spectroscopic redshifts, as a function of I_{814} AB magnitude. The current redshift database is roughly 80% complete to $I = 23$ ($B \approx 24$), but completeness drops rapidly at fainter magnitudes. Stars have been excluded from this figure.

The current redshift database is roughly 80% complete to $I = 23$ ($B \approx 24$), but completeness drops rapidly at fainter magnitudes. Even in the brightness range where the redshift surveys are reasonably complete, there are well-known biases against finding galaxies in the redshift range $1.2 < z < 2.5$. In this range, [OII] λ3727 has shifted into the forest of atmospheric OH lines, and it is not until $z \sim 2.5$ that prominent UV features such as CIV λ1550 and Lyα become accessible

to the red-sensitive LRIS spectrograph on the Keck telescope. The situation will improve with new instrumentation, but some incompleteness in this redshift range is probably an unavoidable problem for ground-based telescopes.

Spectroscopic redshifts are available for less than 5% of the detected sources in the HDF. One of the major uses of the spectroscopic redshifts has been to test "photometric redshifts," which use colors to assign a likely redshift to each galaxy in the field (Connolly et al. 1997; Lanzetta, Yahil, & Fernández-Soto 1996; Mobasher et al. 1996; Sawicki, Lin, & Yee 1997; Gwyn & Hartwick 1996). Photometric redshifts can be assigned to much fainter magnitudes than spectroscopic redshifts, and probably do not suffer the same bias against the $1.2 < z < 2.5$ redshift range. Different techniques have been used by different groups. Most of the published works use the four-band observations of the HDF and rely on fitting spectral energy distribution (SED) templates to the observed colors, shifting both galaxy type and redshift to find the best fit. The fitting procedure used by Gwyn & Hartwick (1996) and Mobasher et al. (1996) did not include the attenuation by intergalactic HI (Yoshii & Peterson 1994; Madau 1995).

The new spectroscopic redshifts obtained during the 1997 observing season made possible a "blind" test of the photometric redshift predictions (Hogg et al. 1998). This test showed good agreement with spectroscopic redshifts for all the groups, with more than 68% of the sources agreeing with spectroscopic redshifts to within $|\Delta z| < 0.1$. Lanzetta, Fernández-Soto, & Yahil (1998) point out that in the case of discrepancies, it is sometimes the *spectroscopic* redshift that is in error.

By the time of the blind test most of the different groups had modified their techniques to include intergalactic absorption, and several groups were taking advantage of the ground-based near-IR (J, H, and K band) photometry for the brighter galaxies. Thus the comparison does not give a fair test of the reliability of the *published* analyses. Of course, given the incompleteness limits of the spectroscopic database, the blind comparison also does not test the photometric redshifts fainter than $I \sim 23$, or in the redshift range where the spectroscopic surveys provide no data.

One of the aims of photometric redshifts is to provide information on the galaxy redshift distribution at faint magnitudes. In this regard, comparison of the published photometric redshift distributions is rather discouraging. While there is broad agreement among the different studies that the majority of galaxies with $I_{814} < 27$ have redshifts $z < 2$, the details differ quite a bit. A comparison of the redshift distributions of Gwyn & Hartwick (1996; GH96) and Lanzetta et al. (1996; LYF96) (both catalogs are available on the World-Wide-Web) provides an example. For $24 < I_{814} < 27$ the surface densities of galaxies at $z < 1$ in the two catalogs agree to within 1%. However, at higher redshifts the ratios of the surface densities LYF96/GH96 are 2.8, 0.5, 1.0, 5.0 for galaxies with $z = 1.5, 2.5, 3.5(\pm 0.5)$, and $z > 4$, respectively. The GH96 distribution has a pronounced bimodal shape (reminiscent of the dwarf-dominated model of Babul & Ferguson 1996), which Sawicki et al. (1997) attribute to the choice of galaxy templates and the neglect of IGM attenuation. The differences in the redshift distributions at faint magnitudes for catalogs which match the spectroscopic redshifts at bright magnitudes suggests that

photometric redshifts (at least in the published versions) are not yet robust enough to use for testing galaxy evolution models much beyond the spectroscopic limit.

Another type of "photometric redshift" is color selection via the Lyman break (Clements & Couch 1996; Madau et al. 1996; Lowenthal et al. 1996). This procedure does not attempt to assign a redshift to every galaxy in the image, but instead identifies those galaxies that are likely to be at high redshift. The use of the technique is discussed in more detail in §5.

3.5 Galaxy Kinematics

Kinematics have been measured for a few subsamples of galaxies in the HDF and flanking fields. Vogt et al. (1997) observed a sample of 8 well-resolved disk galaxies with $I_{814} < 22.1$ in the HDF flanking fields. They estimate peak velocities from their spectra and examine the Tully-Fisher relation for galaxies at modest redshift $0.3 < z < 0.75$. The slope of the relation is found to be the same as for local samples, but there is an offset of about 0.4 mag in the sense that higher-redshift galaxies are brighter than their nearby counterparts. The offset is presumably caused by luminosity evolution and does not correlate with galaxy mass for galaxies in their sample.

Phillips et al. (1996) and Guzman et al. (1996) selected objects likely to be compact star-forming galaxies. They find spectra typical of starburst galaxies (as opposed to AGN), and line-widths ranging from $\sigma \sim 35$ to $150\,\mathrm{km\,s^{-1}}$. Star-formation rates measured from [O II] 3727 range from 0.1 to 14 $M_\odot\,\mathrm{yr}^{-1}$. While such low-mass galaxies make up only $\sim$ 20% of the field population, they may contribute as much as ~45% to the global star-formation rate of the universe at $0.4 < z < 1$.

3.6 Infrared and Radio sources

Extensive followup observations in the near-infrared J, H and K bands have been carried out by Dickinson (1998b) and Hogg et al. (1997), resulting in detection of roughly 300 sources. These data have been used to refine photometric redshift estimates (see §3.4), to study the colors of Lyman-break galaxies (Dickinson 1998a) and to set constraints on the density of passively-evolving elliptical galaxies at high redshift (Zepf 1997; Franceschini et al. 1997). Followup observations with the NICMOS camera on HST are expected in 1998.

The HDF was observed by the Infrared Space Observatory in June and July 1996, and again in July 1997. The ISOCAM camera was used at $6.7\mu m$ and $15\mu m$. A handful of sources were detected in the HDF central field, and a few more in the flanking fields (Serjeant et al. 1997; Goldschmidt et al. 1997; Oliver et al. 1997). Source detection is a difficult problem in the ISO images due to the relatively low spatial resolution and signal-to-noise ratio. It is often difficult to identify a single galaxy responsible for the infrared emission, and many of the reported ISO sources are marginal detections. Mann et al. (1997) attempt to associate the ISO sources with optical sources detected in the HDF. Rowan-Robinson et al. (1997)

use the 13 most reliable identifications, together with model SEDs and photometric redshifts from Mobasher et al. (1996), to derive star-formation rates of 8-1000 $M_\odot\,\mathrm{yr}^{-1}$ for the detected sources, and infer a $60\mu m$ luminosity-density at $0.5 < z < 1$ about a factor of two higher than that inferred from the optical source counts. The conclusion is unfortunately quite sensitive to the reliability of the optical identifications and photometric redshifts, to the reality of the ISO sources near the sensitivity limit, and to the starburst models assumed for the SEDs.

Observations of the HDF with the BIMA array (Wilner & Wright 1997) to a sensitivity of 0.7 mJy reveal no sources. This result suggests that are no objects in the HDF, out to redshifts $z > 20$, with star-formation rates in excess of $\sim 1000\,M_\odot\,\mathrm{yr}^{-1}$. None of the ISO sources are detected. The current, somewhat conflicting, results highlight the need for higher sensitivity observations in the far-IR, sub-mm and millimeter wavebands.

Deep observations of the HDF have been carried out with the VLA (Fomalont et al. 1997) and the MERLIN arrays. These observations extend previous work on micro-Jansky radio sources in the next-deepest HST field (Windhorst et al. 1995), which suggest that many of these sources are star-forming or post-starburst galaxies at modest redshifts. Richards (1998) discusses the 31 sources detected in the HDF and flanking fields, together with the results from other deep fields. Most of the sources are associated with relatively luminous galaxies at a typical redshift $z \sim 0.8$. There is a large dispersion in colors, radio luminosities and emission line strengths for the detected sources, suggesting that the micro-Jansky population is a mixture of low-luminosity AGN, starburst, and post-starburst objects. Two of the detected sources are $z \sim 3$ Lyman-break galaxies. The rest-frame UV spectra are typical of star-forming galaxies, with fluxes suggesting star-formation rates of 20-50 $M_\odot\,\mathrm{yr}^{-1}$. However, if the radio emission is due to star formation alone and not an AGN, it is likely that the star-formation rate is in the range $500 - 1000\,M_\odot\,\mathrm{yr}^{-1}$.

There is one VLA source that is unidentified to the limits of the HDF. A possible explanation is that this source has a redshift $z > 6$. NICMOS followup observations have been taken to search for the source in the near-IR.

3.7 Gravitational Lensing

The HDF has been used to study both weak and strong lensing of distant galaxies. Hogg et al. (1996) identify candidate strong lens systems, but the lensing possibility is not confirmed by spectroscopy (Zepf, Moustakas, & Davis 1997) and remains a plausible possibility only for one candidate. Dell'Antonio & Tyson (1996) examine the statistics of image shapes of faint background galaxies located near brighter foreground galaxies. The background/foreground separation is statistical and is based on a magnitude and color cut rather than on spectroscopic or photometric redshifts. The result is a 3σ detection of shear of the background population due to the foreground galaxies. This corresponds to a typical mass of $6 \times 10^{11}\,h^{-1}\,M_\odot$ within $20\,h^{-1}\,\mathrm{kpc}$, or a typical $M/L_V \approx 11$ within $10\,h^{-1}\,\mathrm{kpc}$. A similar study was carried out by Hudson et al. (1997) using photometric redshifts. The result is used to derive a constraint on the Tully-Fisher relation at moderate redshift, which sug-

gests that spiral galaxies at fixed circular velocity are roughly a magnitude fainter in the B band at $z \sim 0.6$. This result is found to be consistent with the -0.4 mag brightening to $< z >= 0.5$ reported by Vogt et al. (1997) in the kinematic studies, once the different choices of comological parameters and inclination corrections are accounted for. However, the Hudson et al. (1997) result is inconsistent with the Lilly et al. (1998) interpretation of the evolution of large spiral galaxies in deep redshift surveys.

Villumsen, Freudling, & da Costa (1997) estimate that lensing due to intervening large-scale structure could have a significant influence on the angular correlation function of faint galaxies in the HDF. The HDF itself is too small to provide a useful measurement of this effect, but weak shear measurements and clustering measurements in wider HST fields will soon become important cosmological tools.

3.8 Galaxy Clustering

The HDF provides the opportunity to measure the clustering properties of faint galaxies, both as a whole and in different classes separated by photometric redshift. The angular correlation function $\omega(\theta)$ for the 1700 brightest objects in the field was measured by Villumsen et al. (1997). They find that at faint magnitudes the clustering amplitude continues to decrease but at a slower rate than predicted by the power law $\omega(1") \propto 10^{-0.27R}$ observed for shallower samples. With their assumed redshift distribution, the authors conclude that linear evolution in clustering would produce a population with present-day correlation length similar to that measured for IRAS galaxies. Roukema & Valls-Gabaud (1997), using photometric redshifts from Sawicki et al. (1997), estimate that the typical co-moving separations that contribute most of the angular correlation for $I_{814} < 27$ are well below 1 Mpc. Thus the angular correlation function may probe structure on the scale of galaxy halos rather than the large-scale structure.

Colley et al. (1996) considered separately a subset of galaxies selected by color to be at redshifts $z > 2$. They find that the correlation amplitude increases by nearly an order of magnitude at 1" and suggest (Colley et al. 1997) that many individual clumps at this separation are part of the same larger galaxy. Ferguson (1998) compared different HDF catalogs and noted that at small angular separations the details of the splitting and merging of objects are highly sensitive to the algorithms used to make the catalog. If these difficulties can be surmounted, the angular clustering properties of color-selected high-z galaxies offer an interesting probe into galaxy formation. Evidence is mounting that the general population selected on the basis of Lyman breaks is strongly clustered (Steidel et al. 1998; Giavalisco et al. 1998). Within the context of Cold-Dark-Matter (CDM) models, this would be indicative of a high bias factor, as expected from the low co-moving density of sources (Mo & Fukugita 1996; Ogawa, Roukema, & Yamashita 1997; Governato et al. 1998; Coles et al. 1998).

4 Galaxy Evolution Models

I have yet to see any problem, however complicated, which, when you look at it the right way, did not become still more complicated. (Poul Anderson)

The growing body of data on the HDF and other deep fields presents a challenge to models of galaxy evolution. The task is to account for the complete distribution of sizes, shapes, surface-brightness profiles, magnitudes, colors, and clustering properties of the galaxies detected. This should ideally be done with a model that can reproduce the known distributions of such properties in the nearby universe. The ultimate challenge is to construct such models purely from physical principles. However, in the attempt to identify broad trends in the evolution it is often useful to compare to models with various parametrized forms of evolution, or with no evolution at all.

The mechanics of computing models for the distribution of faint galaxies are outlined in Sandage (1988) and Yoshii & Takahara (1988). The procedures involve accounting for the shifting and stretching of the galaxy spectrum due to redshift (the $k(z)$ correction), and the evolution of each galaxy's intrinsic spectrum (traditionally called the $E(z)$ correction). Models that include merging need to track the evolution of the co-moving density of galaxies and the evolution of the mass function. Models that attempt to match the images in detail must also account for size evolution, the evolution of separate components of galaxies (e.g. bulges and disks), and the selection effects of the survey. The comparisons to models have been treated in different ways by different authors, making it at times difficult to sort the successes from the failures.

4.1 Number Counts

Before commenting on models, it is worth mentioning briefly the different efforts at cataloging the HDF sources. Numerous catalogs have been constructed (Lanzetta, Yahil, & Fernández-Soto 1996; Colley et al. 1996; Sawicki, Lin, & Yee 1997; Dell'Antonio & Tyson 1996; Couch 1996; Metcalfe et al. 1996; Williams et al. 1996; Elson, Santiago, & Gilmore 1996). A few are available on the Web (Lanzetta, Yahil, & Fernández-Soto 1996; Couch 1996; Williams et al. 1996). Different algorithms have been used to construct the catalogs, but all at some level rely on smoothing the image and searching for objects above surface brightness threshold set by the background noise. Ferguson (1998) compared a few of the available catalogs and found reasonable agreement brighter than $V_{606} = 28$, with systematic differences in magnitude scales of less than 0.3 mag (nevertheless, there *are* systematic differences at this level). The different catalogs apply different algorithms for splitting and merging objects with overlapping isophotes. These differences, together with the different schemes for assigning magnitudes to galaxies, result in overall differences in galaxy counts. At $I_{814} = 26$ the galaxy counts in the catalogs considered by Ferguson (1998) all agree to within 25%, while at $I_{814} = 28$ there is a factor of 1.7 difference between the deepest and the least deep catalog. These differences

highlight the fact that galaxy counting is not a precise science. Attempts to fit the number–magnitude relation to better than a factor of 1.5 accuracy should include image simulations and photometry with the same algorithms used to analyze the data.

At very faint magnitudes, it is clear that the HDF counts must miss some galaxies. Vogeley (1997) examines the autocorrelation function of the sky background and estimates that undetected galaxies with sizes and clustering similar to the observed galaxies could provide only about 10% more flux than already seen in detected galaxies. Nevertheless, after careful treatment of different sources of detector, zodiacal, and Galactic backgrounds Bernstein (1997) estimates that the extragalactic background is at least 2-3 times higher than the integrated flux in published galaxy counts. Reconciling the two measurements would require extended halos of the presently detected galaxies, possibly together with a population of very extended, low-surface objects. However, the need for a smooth component must be regarded as tentative given the difficulty in measuring the absolute level of the extragalactic background light.

4.2 No-Evolution Models

The assumption of no evolution is not physically reasonable, but provides a useful fiducial for identifying how much and what kinds of evolution are required to match faint-galaxy data. Traditional no-evolution models are based on estimates of the $z = 0$ luminosity functions for different types of galaxies. The number–magnitude relation is determined entirely by the k corrections and the change in the cosmological parameters as they act through the luminosity distance and the volume element as a function of redshift. The HDF counts exceed the predictions of such models by large factors. Even a very open model ($\Omega_M = 0.02, \Omega_\Lambda = 0$), underpredicts the counts at $I_{814} = 27$ by a factor 3 (Ferguson 1998), as shown in Fig. 5.

Bouwens, Broadhurst, & Silk (1997) construct a non-evolving model from the HDF itself, using 32 galaxies brighter than $I_{814} = 22.3$ to define a fiducial sample. They construct Monte-Carlo realizations of the HDF that might be seen from a universe uniformly populated with such galaxies, shifted to different redshifts and k-corrected on a pixel-by-pixel basis. This kind of simulation automatically incorporates the selection and measurement biases of the HDF at faint magnitudes. It also normalizes the model *by fiat* to match the counts at $I_{814} = 22.3$, where traditional no-evolution models, normalized to the local luminosity function, already encounter serious problems. The resulting models underpredict the HDF counts at $I_{814} = 27$ by factors of 4 and 7 for models with $\Omega_M = 0.1$ and 1.0 (with $\Omega_\Lambda = 0$), respectively. The angular sizes of galaxies in the models are also too big at faint magnitudes, with a median half-light radius about a factor of 1.5 larger than observed for galaxies with $24 < I < 27.5$.

Because the typical redshift of the template galaxies in this model is $z \sim 0.5$, this model comparison suggests that much of the evolution in galaxy number densities, sizes, and luminosities occurs at higher redshift.

The small sizes of faint galaxies essentially rule out low-surface brightness galax-

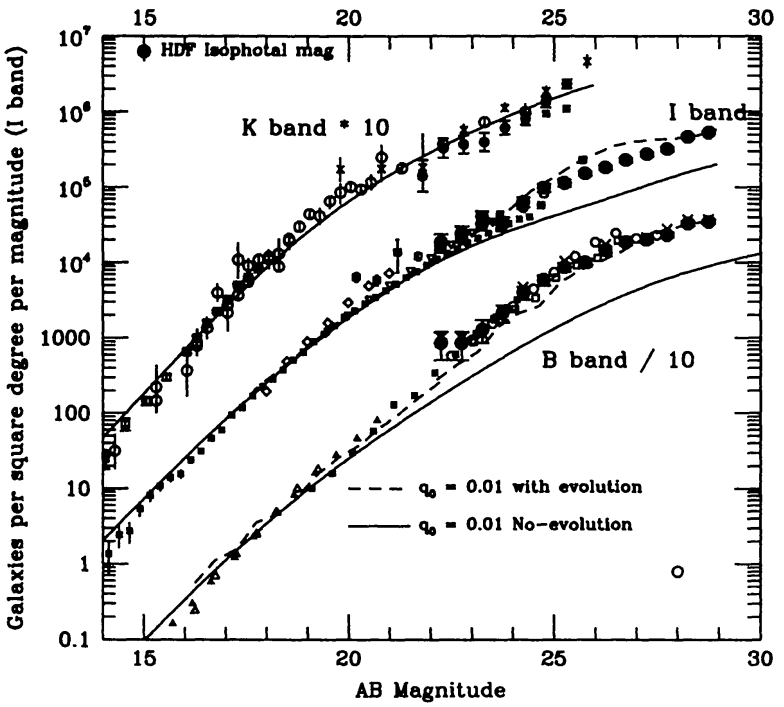

FIG. 5 — HDF counts from Williams et al. (1996), together with a compilation of counts from ground-based surveys. The solid curves show a non-evolving model with $\Omega_M = 0.02$ and $\Omega_\Lambda = 0$ based on the Coleman et al. (1980) spectral energy distributions and the Babul & Ferguson (1996) morphological mix. The dashed curves show a $\Omega_M = 0.02$ PLE model. This model assumes a redshift of formation $z_f = 5$ for all morphological types, with different star-formation timescales for each type. The counts shown for the model are determined from simulated HDF images, and include the effects of surface-brightness dimming and isophotal selection.

ies (Ferguson & McGaugh 1995; McLeod & Rieke 1995) as a significant contributor to the counts at magnitudes $I_{814} > 20$.

4.3 Pure-Luminosity Evolution Models

The next step up in complexity from no-evolution models are the so-called pure-luminosity evolution (PLE) models (Tinsley 1978; Yoshii & Takahara 1988; Yoshii & Peterson 1995; Pozzetti, Bruzual, & Zamorani 1996). These share with no-evolution models the assumptions for galaxy properties in the local universe, but include prescriptions for the evolution of galaxy spectral-energy distributions with time. These prescriptions are generally tied to local constraints on star-forming histories and metallicities obtained from color-magnitude diagrams and integrated

spectra of nearby galaxies. Most PLE models adopt simple parametrized forms for the star-formation histories, use canonical initial-mass functions for stars, and do not model evolution as a function of position within each galaxy. Only a few such models include evolution of metal abundance with time, in all cases based on one-zone models.

PLE models are clearly oversimplified, but once again are useful as a fiducial for assessing what other kinds of evolution are necessary. The neglect of merging in such models is not a serious impediment to modeling galaxy counts. If merging preserves luminosity (i.e. if no additional star-formation is associated with the merging event), then the effect of merging is to slightly steepen the galaxy counts at the faint end. Additional luminosity evolution (presumably associated with the merging) needs to be included to increase the counts significantly.

Metcalfe et al. (1996) compare several different models to the counts and colors of galaxies in the HDF and in deep images taken at the William Herschel Telescope. The cosmological models considered have $\Omega_M = 0.1$ and $\Omega_M = 1$ and no cosmological constant. Redshifts of formation $z_f = 7$ and 10 are assumed, respectively, for the two cases. For low Ω a reasonable fit to $I \approx 26$ is achieved, but the model progressively underpredicts the counts to fainter magnitudes. Several pecularities of the model should be noted. For elliptical galaxies, a heavily dwarf-dominated IMF $x = 3$ is adopted, with a fairly long star-formation timescale ($\tau = 2.5$ Gyr). These assumptions make the formation phase of elliptical galaxies much less luminous than the standard assumptions of Salpeter IMF and $\tau < 1$ Gyr. However, it seems unlikely that such a dwarf-dominated IMF and long star formation timescale can reproduce the metal abundances (and in particular the high ratio of $\alpha-$capture elements relative to iron) in local ellipticals. Another notable feature of the model is the normalization, which is fixed to match the galaxy counts at $B \approx 18$.

For $\Omega_M = 1$ even these adjustments fail to produce a reasonable fit to the data. To attempt to force a fit, Metcalfe et al. (1996) introduce a population of dwarf galaxies that form stars at a constant rate until $z = 1$ and then stop abruptly. While a good fit to the number counts is achieved, the fit to the $V_{606} - I_{814}$ vs. $B_{450} - V_{606}$ color distribution is not as good as for the low-Ω model. The details of the mass function and other properties of this hypothetical dwarf population have not been published. However, it is worth noting that the form of evolution, while justified on the basis of the Babul & Rees (1992) "disappearing-dwarf" model, is quite different from that theoretical prediction. In the Babul & Rees (1992) model, star formation in dwarf galaxies is delayed until *after* $z = 1$ due to photoionization by the UV background.

Based on comparison of the observed color distribution to the PLE models, Metcalfe et al. (1996) conclude that many of the objects in the HDF are at $z \approx 2$.

Another set of PLE models was considered by Pozzetti et al. (1998). The goal of these models was to investigate the constraints on models imposed by the deep near-UV counts, which was one of the main innovations of the HDF. From color-magnitude relations and a study of the fluctuations in the counts in the different HDF bands Pozzetti et al. (1998) conclude that at $B_{450} = 27$ roughly 30% of the sources in the HDF are at $z > 2$. The PLE model considered has $\Omega_M = 0.1$ with

no cosmological constant, and with a redshift of formation $z_f = 6.3$. This model matches the counts quite well but predicts that about 80 objects brighter than $V_{606} = 28$ should disappear from the F450W band due to their high redshift, while in the actual data there are only about 15 such sources.

Ferguson & Babul (1998) considered another low$-\Omega$ PLE model and encountered similar problems. While the galaxy counts and size distribution match the predictions reasonably well, the observed color distribution shows few galaxies with the extreme breaks expected for high-redshift galaxies. Because bulges in this model are assumed to form at high redshifts, the surface density of high-redshift objects is particularly high. The model predicts roughly 400 B-band Lyman-break objects compared to the 15 or so observed.

A problem common to nearly all PLE models is the paucity of objects in the HDF that, based on colors, are likely to be at redshifts $z > 3.5$. PLE models predict a luminous phase of evolution for early-type galaxies and spiral bulges that should be difficult to miss at the depths of the HDF. It may be possible to hide this phase of evolution with large amounts of dust or with an unusual IMF, but such models may run into problems with the infrared background or with the metallicities of local galaxies. Even if the luminous star-forming phase of elliptical galaxies can be somehow hidden, as the dust clears the galaxies should gradually merge with the "passively evolving" tracks expected for a population that is not continuously forming stars (Bruzual & Charlot 1993). However, there are few if any objects in the HDF (and other fields) with colors consistent with passively evolving ellipticals at $z > 1.3$ (Franceschini et al. 1997; Zepf 1997).

4.4 Models with Additional Galaxy Populations

The great difficulty in achieving a fit with $\Omega_M = 1$, even to ground-based galaxy counts, motivated investigations into different kinds of galaxies that might be missed from the census of the local universe but could contribute to the counts of galaxies at faint magnitudes (Ferguson & McGaugh 1995; Babul & Ferguson 1996; Koo, Gronwall, & Bruzual 1993; McLeod & Rieke 1995). Perhaps the most physically motivated of these more exotic possibilities is the idea that the formation of stars in low-mass galaxy halos could be inhibited until low redshifts $z \lesssim 1$ due to photoionization by the metagalactic UV radiation field (Efstathiou 1992; Babul & Rees 1992). The formation of dwarf galaxies at moderate redshifts, in intense bursts of star-formation terminated by supernova-driven winds, provides a plausible way to reconcile $\Omega_M = 1$ models to faint galaxy counts, and the CDM halo mass spectrum to the local galaxy luminosity function. Ferguson & Babul (1998) compared the predictions of such a "disappearing dwarf" model in detail to the HDF. They found that the simplest version of the model (a) overpredicts the counts at faint magnitudes, and (b) overpredicts the sizes of very faint galaxies. These problems are caused by the fact that, for a Salpeter IMF, the dwarfs fade too slowly and would still be visible in great numbers in the HDF at redshifts $z < 0.5$. Such problems could probably be avoided by adopting an IMF skewed toward massive stars. However, the color distributions of the HDF galaxies as a

whole do not favor models where the majority of the population is at $z < 1$, which is the unalterable prediction of such models. Nevertheless the problems in fitting the counts with dwarf-dominated $\Omega_M = 1$ models do not rule out the possibility that photoionization plays a role in governing dwarf-galaxy evolution.

The problems encountered in fitting rapid dwarf-galaxy evolution models to the HDF led Campos (1997) to consider a model with much milder evolution. Dwarfs in this model are assumed to form in less violent episodes, that repeat multiple times per galaxy. As in the Babul & Ferguson (1996) model, star-formation in dwarfs is delayed until $z \sim 1$. To avoid producing too many nearby faded dwarfs, each star-formation episode must be relatively long (a few times 10^8 years). Acceptable fits to the counts and colors of galaxies are achieved both for high and low values of Ω. At faint magnitudes the models are dominated by galaxies with redshifts $z < 0.8$. This could in principle be tested with observations of the HDF at wavelengths farther into the UV.

4.5 Semi-Analytic Hierarchical Models

Semi-Analytic models (White & Rees 1978; White & Frenk 1991; Kauffmann, Guiderdoni, & White 1994) offer a promising way to attach the basic physics of galaxy formation to the evolution of structure predicted by hierarchical models. Various prescriptions for gas cooling, star-formation, feedback, and merging are used to predict galaxy properties as a function of redshift. These prescriptions are tuned to provide a reasonable match to properties of galaxies in large halos at the present epoch.

Baugh, Cole, & Frenk (1996) compare the predictions of one such model to galaxy counts as a function of morphological type in the HDF and MDS surveys. The model follows the merging history of dark-matter halos using Monte-Carlo techniques. The gas associated with each dark-matter halo virializes soon after halo collapse and then cools radiatively. Left alone, the gas is assumed to settle into a disk, and will form stars at a rate regulated by the mass of cool gas and the feedback from supernovae and stellar winds. When a merger of two halos occurs, the hot gas of the two progenitors is assigned to the new larger halo, and the slow merging of the cold gas and star components in governed by dynamical friction. This particular model is unable to reproduce simultaneously the local galaxy luminosity function and the zero-point of the Tully-Fisher relation (Cole et al. 1994), although with some fine-tuning semi-analytic models may be able to pass this test (Somerville & Primack 1998).

Morphological types in the Baugh, Cole, & Frenk (1996) model are assigned via a simple prescription based on bulge/disk ratio. If a galaxy has experienced a violent merger within the 1 Gyr prior to the "observation" it is classified as a peculiar galaxy. The parameters dividing the morphological classes are tuned to reproduce the local morphological mix of galaxies. The resulting model is able to reproduce separately the number–magnitude relation for E/S0 galaxies, spirals and irregular/peculiar galaxies down to $I_{814} = 24$, with an $\Omega_M = 1$ standard CDM cosmology. The model has not yet been tested in detail to fainter magnitudes.

5 Lyman-Break Galaxies

Perhaps the most important change in the faint-galaxy landscape in the last three years has been the identification of a significant population of high-redshift ($z > 2$) star-forming galaxies (Steidel, Pettini, & Hamilton 1996; Steidel et al. 1996b). The combined effects of intrinsic Lyman-continuum absorption, and absorption due to intergalactic HI, produce a pronounced break in the spectral energy distributions of galaxies at a rest-frame wavelength of 912Å. For redshifts $z < 3$ most of the effect is due to the Lyman edge intrinsic to galaxies. From stellar atmospheres alone, a factor of 3 discontinuity is expected. Any additional HI in the galaxy will increase this factor. No emission from below the Lyman break has been detected from local starburst galaxies; typical upper limits suggest that less than 5% of the photons at $\sim$ 900Å escape (Leitherer et al. 1995; Hurwitz, Jelinsky, & Dixon 1997). The combined effects suggest that the typical intrinsic Lyman-edge discontinuity will be more than four magnitudes. Superimposed on this is the absorption from the Lyman alpha forest. For galaxies at $z < 3$ the major intergalactic contribution is near and beyond the Lyman limit. The decrement due to the Lyα lines alone is roughly 30%. At higher redshifts, the decrement due to Lyα lines starts to become more significant.

Various groups have used color selection to identify high-redshift galaxies in the HDF (Clements & Couch 1996; Madau et al. 1996; Lowenthal et al. 1996; Dickinson 1998a). The selection criteria and magnitude limits vary, leading to different numbers of Lyman-break candidates in the different samples. To date 26 galaxies in the HDF have spectroscopic redshifts $z > 2$. Of these, 23 were identified via color selection.

The properties of the spectroscopically confirmed high-redshift galaxies are summarized by Lowenthal et al. (1996), Dickinson (1998a) and Pettini et al. (1997). The Keck observations cover the rest-frame far-UV portion of the spectra. The spectra are similar to the integrated continuum of O and B stars, punctuated by strong interstellar absorption lines. In at least a few systems there is evidence that the interstellar lines are blueshifted relative to weak photospheric lines in the O stars, suggestive of bulk outflows of the interstellar medium. The metallicities of the galaxies are not easily determined, but the strengths of the stellar wind lines are typically weaker than seen in nearby high-metallicity starburst galaxies; Lowenthal et al. (1996) suggest that stars in the SMC are the most similar local analogy. Measurements of velocity dispersions or rotation curves for Lyman-break galaxies are extremely difficult. Preliminary indications from infrared spectroscopy of optical Hβ and [OIII] emission lines suggest modest velocity dispersions $\sigma \sim 70\,\mathrm{km\,s^{-1}}$. The morphologies of the objects vary, but most are compact, with half-light radii $r_{hl} \sim 3.6 h_{50}^{-1}$kpc, comparable to present-day small elliptical galaxies and spiral bulges. There are few if any Lyman-break galaxies that morphologically resemble present-day disk galaxies. However, typical present-day disks with modest star-formation rates would be below the HDF detection limits at $z > 2$, so we cannot say that they do not exist at these redshifts. With no correction for extinction, the star-formation rates of the spectroscopically confirmed Lyman-break galaxies in the HDF range from 4 to 20 $M_\odot\,\mathrm{yr}^{-1}$. For the fainter photometric sample identified

by Madau et al. (1996) the faintest objects have nominal star-formation rates of $\sim 1\,M_\odot\,\mathrm{yr}^{-1}$, for a Salpeter IMF with an upper-mass cutoff of $100\,M_\odot$. Possible corrections for extinction are discussed below.

6 The Integrated Star-Formation History of the Universe

The Universe is like an aging professor with his brilliant future behind him. (Attributed to Allan Sandage)

The integrated flux in the Lyman-break objects can be used to set constraints on the total amount of star-formation and metal production at high redshift. Estimates of the star-formation rate depend strongly on the assumed initial mass function. Estimates of the metal production rate are less sensitive to the IMF because the same massive stars that produce most of the metals through type II SNe also produce most of the UV radiation detected by the HDF.

Initial estimates of the metal production rate vs. redshift were based on an Hα survey at low redshift (Gallego et al. 1995), the estimated rest-frame luminosity at 2800Å for galaxies at moderate redshift (Lilly et al. 1996), and the estimated rest-frame 1500 Å luminosity at redshifts $z > 1$. The first estimate for galaxies at $z > 1$ was derived from the statistics of color-selected high$-z$ objects in the HDF by Madau et al. (1996). They estimated that the metal production rate at $z \approx 2.8$ is approximately 3 times higher than the local rate, but 4 times lower than the rate at $z \approx 1$.

The Madau et al. (1996) estimate is best regarded as a *lower limit* to the metal production rate. There are several corrections that should be applied to obtain a more realistic estimate of the true metal production rate. First, the Madau et al. (1996) galaxy magnitudes were isophotal. Conversion to true total magnitudes is uncertain, but is likely to increase the luminosity density by a factor of 1.5. Second, no extrapolation of the luminosity function was made to account for sources below the detection limit. The sources span about a factor of 10 in luminosity. If we assume that the sample spans the range from 0.5 to $5 \times L^*$, extrapolating to galaxies 10 times fainter would increase the luminosity density by factors of 1.6 or 2.0 for Schechter (1976) luminosity functions with slope $\alpha = -1$ and -1.3, respectively. Third, the typical galaxy is not likely to be dust-free. The extinction correction is extremely uncertain, but is likely to increase the metal-production rate estimated from the 1500Å luminosity density by at least a factor of two (see below).

The end result is a likely factor of ~ 5 increase in the metal-production rate at $z > 2$ over Madau et al. (1996) lower limits. This will raise the $z \approx 2.8$ metal-production rate close to the Lilly et al. (1996) rate at $z \sim 0.8$, but that value would also move higher if corrected for extinction.

Sawicki et al. (1997) and Connolly et al. (1997) use photometric redshifts to estimate the metal-formation rate down to lower redshifts than possible from Lyman-break galaxies alone. The estimates agree well with the Lilly et al. (1996) estimate. None of these studies include a treatment of dust. The Sawicki et al.

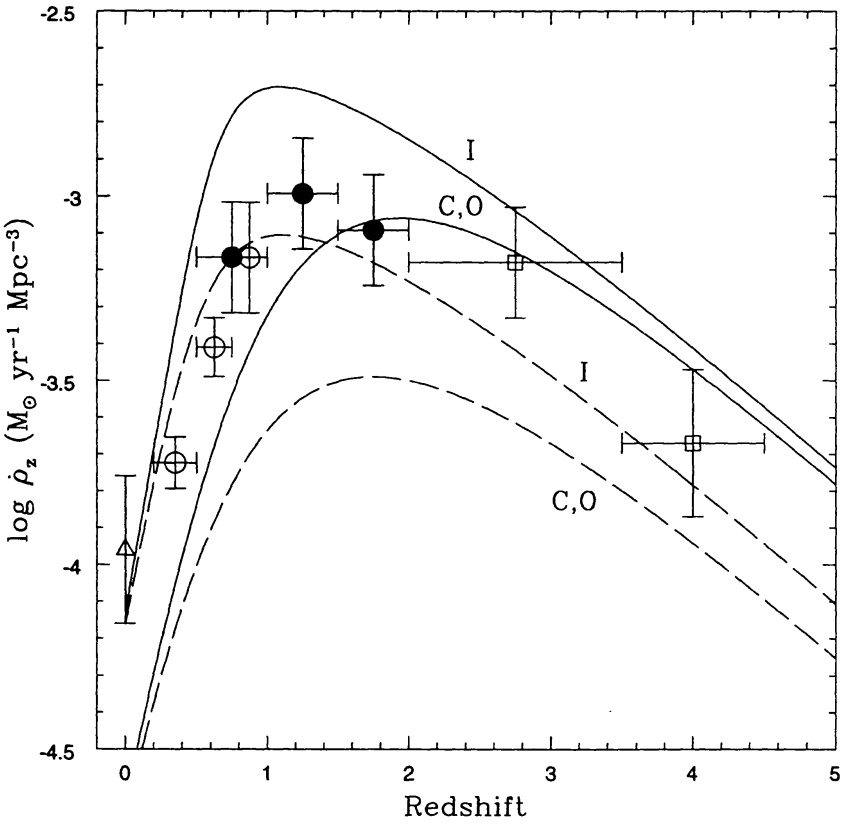

FIG. 6 — The global metal enrichment rate as a function of redshift. The symbols are as follows: open triangle – Gallego et al. (1995); open circles – Lilly et al. (1996); filled circles – Connolly et al. (1997); open squares – Madau et al. (1996). The photometric redshift luminosity densities have been corrected for incompleteness assuming a Schechter luminosity function with a slope $\alpha = -1.3$. The solid and dashed lines represent the predictions of Pei & Fall (1995) for the metal enrichment rate based on damped Lyα absorption-line systems. From Connolly et al. (1997).

(1997) estimates at high-redshift are significantly higher than those of (Madau et al. 1996) but include the extrapolation to total magnitudes and the extrapolation down the luminosity function.

The results from Connolly et al. (1997) and Madau et al. (1996) are summarized in Fig. 6. The peak in the metal-production rate (or star-formation rate) at $z \approx 1-2$ is similar to that previously inferred from an analysis of damped Lyman-α absorption line systems by Pei & Fall (1995), also shown in Fig. 6. It is also similar to that predicted by the semi-analytic hierarchical models of (Baugh et al. 1997). However, it is not a unique prediction of such models. Totani, Yoshii, & Sato (1997) obtain a similar metal-formation history for $z < 1$ for PLE models involving a cosmological constant, although the peak at $z > 3.5$ predicted must be somehow missed by the HDF for the model to be considered viable.

There are two important corrections to the high-z star-formation rate that are

potentially larger than the small factors mentioned above. The first is the correction for exinction. Comparing the observed spectral-energy distributions of Lyman-break galaxies to those of nearby starburst galaxies, Meurer (1998) estimates that the median obscuration factor is a factor of ~ 10. Sawicki & Yee (1998) arrive at a correction factor of ~ 20 based on comparison to model spectral energy distributions. In both cases the correction factor is derived from the Calzetti, Kinney, & Storchi-Bergmann (1994) "obscuration" curve, which is empirically derived for local starburst galaxies. Dickinson (1998a) points out that smaller correction factors are required for the same amount of extinction with a foreground screen model with the SMC extinction curve. None of these correction factors include the effect of missing galaxies entirely due to dust attenuation.

The uncertainties in the correction factors are large enough that the downturn in the metal formation rate at $z > 3$ must be regarded as tentative. It is true that the corrections for extinction are likely to be similar for the Lyman-break selected sample. If anything, they might be expected to decrease at the highest redshifts where young metal-poor galaxies presumably are the norm. However, it is also likely that selection effects due to surface-brightness detection limits become more important at high redshift (Ferguson 1998).

The predictions of the models must also be regarded as tentative. For the PLE models, the apparent metal-formation at $z > 3$ is a problem, but one that might be surmounted by inclusion of dust obscuration (Franceschini et al. 1994). In the semi-analytic hierarchical models, changing the prescriptions for cooling, star-formation and feedback (within the uncertainties of our knowledge of the physical processes) can probably move the peak to higher redshifts. It remains to be seen whether such changes would improve or destroy the present qualitative agreement with galaxy properties at $z = 0$.

7 Conclusions

The HDF has focused attention on several important problems in galaxy evolution.

Faint blue galaxies. In summarizing the status of the "faint blue galaxy problem" it is important to draw the distinction between the relatively bright $I_{814} < 23$ faint galaxies, now probed by spectroscopic surveys, and the very faint faint galaxies $I_{814} > 25$ probed only by images. The total integrated light from the galaxy counts is dominated by galaxies with $I_{814} < 23$ (Pozzetti et al. 1998), most of which have regular morphologies, and luminosities consistent with modest luminosity evolution of the present-day luminosity function. Locally, most of the known stellar mass in the universe is concentrated in large $L \sim L^*$ galaxies. A fairly consistent picture emerges of quiescent evolution of typical $L \approx L^*$ galaxies out to $z \approx 1$. This picture is marred only by the controversial claim of strong density evolution among ellipticals in the CFRS survey (Kauffmann, Charlot, & White 1996).

It is much less clear how to relate $I_{814} > 25$ population to galaxies in the local universe. The blue colors and photometric redshifts suggest that most of these objects are star-forming galaxies at $z < 2$. To match the counts at faint magnitudes, the co-moving density of compact star-forming objects must have been

substantially higher at $z \approx 1$ than it is today. The excess galaxies must either merge into present-day large galaxies, or fade into the very faint end of the local luminosity function.

The paucity of high-redshift star-forming galaxies. While the data out to $z \approx 1$ for galaxies with $I_{814} < 23$ appear to be in reasonable agreement with PLE models, the evidence at higher redshifts appears to contradict them. A common feature of models that do not involve a lot of late-epoch merging is the prediction of a luminous "star-burst" phase among the progenitors of elliptical galaxies and spiral bulges at early epochs. The most obvious evidence against such models is the lack of bright U_{300}, B_{450} and V_{606}-band Lyman-break dropouts in the HDF. The luminosity-density at high redshift is lower than anticipated from the models. It is possible that with substantial corrections for dust and incompleteness, the well-studied $z \approx 3$ population can account for stars in local elliptical galaxies and spiral bulges, but the redshift seems uncomfortably low given the evidence for mild evolution and small scatter in the properties of cluster ellipticals out to $z \approx 1.2$ (Dickinson 1995b; van Dokuum et al. 1998). It seems more likely that many galaxies are hidden at $z > 4$, but there are currently no data to support that view.

Nevertheless, the chemical evidence in favor of rapid chemical enrichment of elliptical galaxies is quite strong (Gibson 1997), and the one bulge (that of our galaxy) for which we can obtain a main-sequence color-magnitude diagram appears similar in age to the galactic halo (Ortolani et al. 1995). While hierarchical models are better able to account for the apparent lack of a luminous proto-galaxy phase, the current semi-analytic models have not yet been able to match both the local constraints and the constraints from faint-galaxy surveys.

The peak in the UV luminosity density at $z \approx 1 - 2$. Studies of the HDF by Madau et al. (1996) and others have popularized the use of figures showing the global metal-enrichment history of the universe (or star-formation history, or evolution in the luminosity density). These diagrams provide a useful tool for putting different surveys into the same context, and for relating the evolution of luminous material to the evolution of gas (Pei & Fall 1995). The apparent peak at $1 < z < 2$ is hotly debated. But the debate itself serves to sharpen our understanding of the difficult interconnections between metal-enrichment, dust, and the evolution of luminous material, and to hone techniques for measuring these things, in both nearby and distant galaxies.

The HDF observation is but one in a long line of surveys. It will soon be superseded by deeper and wider surveys, and by a flood of information at other wavelengths. It is perhaps still too early to assess what lasting impacts the HDF will have on our understanding of distant galaxies. However, the depth and quality of the images, and the new information they provide, has clearly motivated new ways of approaching the studies of faint galaxies. As the deeper surveys supplant the HDF, these new approaches should pave the way to a deeper understanding of the origin of galaxies and the underlying cosmological model.

8 Acknowledgments

I am indebted to my fellow HDF enthusiasts, too numerous to mention, for the many fruitful discussions that have provided input for this review. I thank Bob Williams, in particular, for making the HDF observations possible, and for offering me the chance to participate in the project.

This work was supported by NASA grant AR-06337, awarded by the Space Telescope Science Institute, which is operated by the Association of Universities for Research in Astronomy, Inc., for NASA under contract NAS5-26555.

References

Abraham, R. G. 1997, in The Ultraviolet Universe at Low and High Redshift: Probing the Progress of Galaxy Evolution, ed. W. H. Waller, M. N. Fanelli, J. E. Hollis, & A. C. Danks (Woodbury, New York: AIP), 195

Abraham, R. G., Tanvir, N. R., Santiago, B. X., Ellis, R. S., Glazebrook, K., & van den Bergh, S. 1996, MNRAS, 279, L47

Adams, F. C., & Fatuzzo, M. 1996, ApJ, 464, 256

Alcock, C., et al. 1997, ApJ, 486, 697

Babul, A., & Ferguson, H. C. 1996, ApJ, 458, 100

Babul, A., & Rees, M. 1992, MNRAS, 255, 346

Bahcall, J. N., Flynn, C., Gould, A., & Kirhakos, S. 1994, ApJ, 425, L51

Bahcall, J. N., Guhathakurta, P., & Schneider, D. P. 1990, Science, 248, 178

Baugh, C. M., Cole, S., & Frenk, C. S. 1996, MNRAS, 282, L27

Baugh, C. M., Cole, S., Frenk, C. S., & Lacey, C. G. 1997, submitted

Bernstein, R. 1997, PhD. Thesis. California Institute of Technology

Bouwens, R., Broadhurst, T., & Silk, J. 1997, astro-ph/9710291

Brainerd, T. G., Smail, I., & Mould, J. 1995, MNRAS, 275, 781

Bressan, A., Chiosi, C., & Fagotto, F. 1994, ApJS, 94, 63

Bruzual, A. G., & Charlot, S. 1993, ApJ, 405, 538

Calzetti, D., Kinney, A. L., & Storchi-Bergmann, T. 1994, ApJ, 429, 582

Campos, A. 1997, ApJ, 488, 606

Carroll, S. M., Press, W. H., & Turner, E. L. 1992, ARA&A, 30, 499

Casertano, S., Ratnatunga, K. U., Griffiths, R. E., Im, M., Neuschaefer, L. W., Ostrander, E. J., & Windhorst, R. A. 1995, ApJ, 453, 599

Chabrier, G., & Mera, D. 1997, A&A, 328, 83

Clements, D. L., & Couch, W. J. 1996, MNRAS, 280, L43

Cohen, J. G., Cowie, L. L., Hogg, D. W., Songaila, A., Blandrod, R., Hu, E. M., & Shopbell, P. 1996, ApJ, 471, L5

Cole, S., Aragon-Salamanca, A., Frenk, C. S., Navarro, J. F., & Zepf, S. E. 1994, MNRAS, 271, 781

Coleman, G. D., Wu, C.-C., & Weedman, D. W. 1980, ApJS, 43, 393

Coles, P., Lucchin, F., Matarrese, S., & Moscardini, L. 1998, astro-ph/9803197

Colless, M. M., Ellis, R. S., Broadhurst, T. J., Taylor, K., & Peterson, B. A. 1993, MNRAS, 261, 19

Colley, W., Gnedin, O., Ostriker, J. P., & Rhoads, J. E. 1997, ApJ, 488, 579

Colley, W. N., Rhoads, J. E., Ostriker, J. P., & Spergel, D. N. 1996, ApJ, 473, L63

Connolly, A. J., Szalay, A. S., Dickinson, M., SubbaRao, M. U., & Brunner, R. J. 1997, ApJ, 486, 11

Couch, W. J. 1996, http://ecf.hq.eso.org/hdf/catalogs/

Cowie, L. L., Hu, E. M., & Songaila, A. 1995, Nature, 377, 603

Cowie, L. L., Songaila, A., Hu, E. M., & Cohen, J. G. 1996, AJ, 112, 839

Dell'Antonio, I. P., & Tyson, J. A. 1996, ApJ, 473, L17

Dickinson, M. 1995a, in Galaxies in the Young Universe, ed. H. Hippelein, H.-J. Meisenheimer, & H.-J. Röser (Berlin: Springer), 144

Dickinson, M. 1995b, in Fresh Views on Elliptical Galaxies, ASP Conf Series, ed. A. Buzzoni, A. Renzini, & A. Serrano (San Francisco: ASP), 283

Dickinson, M. 1998a, in The Hubble Deep Field, ed. M. Livio, S. M. Fall & P. Madau, (Cambridge U. Press: Cambridge), in press

Dickinson, M. 1998b, in preparation

Dressler, A., Oemler, A. J., Sparks, W. B., & Lucas, R. A. 1994, ApJ, 435, L23

Driver, S. P., Windhorst, R. A., Ostrander, E. J., Keel, W. C., Griffiths, R. E., & Ratnatunga, K. U. 1995, ApJ, 449, L23

Efstathiou, G. 1992, MNRAS, 256, 43P.

Efstathiou, G., Bernstein, G., Tyson, J. A., Katz, N., & Guhathakurta, P. 1991, ApJ, 380, L47

Elson, R. A. W., Santiago, B. X., & Gilmore, G. F. 1996, New Astron., 1, 1

Fasano, G., Cristiani, S., Arounts, S., & Filippi, M. 1998, astro-ph/9801078

Ferguson, H. C. 1998, in The Hubble Deep Field, ed. M. Livio, S. M. Fall & P. Madau, (Cambridge U. Press: Cambridge), in press

Ferguson, H. C., & Babul, A. 1998, MNRAS, in press

Ferguson, H. C., & McGaugh, S. S. 1995, ApJ, 440, 470

Flynn, C., Gould, A., & Bahcall, J. N. 1996, ApJ, 466, L55

Fomalont, E. B., Kellerman, K. I., Richards, E. A., Windhorst, R. A., & Partridge, R. B. 1997, ApJ, 475, 5

Franceschini, A., Mazzei, P., de Zotti, G., & Danese, L. 1994, ApJ, 427, 140

Franceschini, A., Silva, L., Granato, G. L., Bressan, A., & Danese, L. 1997, astro-ph/9707064

Fruchter, A. S., & Hook, R. N. 1997, in preparation

Fukugita, M., Hogan, C. J., & Peebles, P. J. E. 1997, astro-ph/9712020

Gallego, J., Zamorano, J., Aragon-Salamanca, A., & Rego, M. 1995, ApJ, 455, L1

Giavalisco, M., Steidel, C. C., Adelberger, K. L., Dickinson, M. E., Pettini, M., & Kellogg, M. 1998, astro-ph/9802318

Gibson, B. K. 1997, MNRAS, 290, 471

Glazebrook, K., Ellis, R., Colless, M., Broadhurst, T., Allington-Smith, J., & Tanvir, N. 1995a, MNRAS, 273, 157

Glazebrook, K., Ellis, R. S., Santiago, B., & Griffiths, R. E. 1995b, MNRAS, 275, L19

Goldschmidt, P., et al. 1997, MNRAS, 289, 465

Gould, A., Bahcall, J. N., & Flynn, C. 1996, ApJ, 465, 759

Gould, A., Bahcall, J. N., & Flynn, C. 1997, ApJ, 482, 913

Governato, F., Baugh, C. M., Frenk, C. S., Cole, S., Lacey, C. G., Quinn, T., & Stadel, J. 1998, astro-ph/9803030

Griffiths, R., et al. 1996, in IAU Symposium 168: Examining the Big Bang and Diffuse Background Radiations, ed. M. Kafatos & Y. Kondo (Dordrecht: Kluwer)

Guzman, R., Gallego, J., Koo, D. C., Phillips, A. C., Lowenthal, J. D., Faber, S. M., Illingworth, G. D., & Vogt, N. P. 1996, ApJ, 489, 559

Gwyn, S. D. J., & Hartwick, F. D. A. 1996, ApJ, 468, L77

Hillenbrand, L. A. 1997, AJ, 113, 1733

Hogg, D. W., et al. 1998, AJ, in press

Hogg, D. W., Blandford, R., Kundic, T., Fassnacht, C. D., & Malhotra, S. 1996, ApJ, 467, 73

Hogg, D. W., Neugebauer, G., Armus, L., Matthews, K., Pahre, M. A., Soifer, B. T., & Weinberger, A. J. 1997, AJ, 113, 474

Hudson, M. J., Gwyn, S. D. J., Dahle, H., & Kaiser, N. 1997, astro-ph/9711341

Hunter, D., Light, R. M., Holtzman, J. A., Lynds, R., O'Neil, E. J. J., & Grillmair, C. J. 1997, ApJ, 478, 124

Hurwitz, M., Jelinsky, P., & Dixon, W. V. D. 1997, ApJ, 481, L31

Im, M., Casertano, S., Griffiths, R. E., & Ratnatunga, K. U. 1995, ApJ, 441, 494

Kauffmann, G., Charlot, S., & White, S. D. M. 1996, MNRAS, 283, L117

Kauffmann, G., Guiderdoni, B., & White, S. D. M. 1994, MNRAS, 267, 981

Kerins, E. J. 1997, A&A, 328, 5

Koo, D. C., Gronwall, C., & Bruzual, G. A. 1993, ApJ, 415, L21

Kormendy, J. 1985, ApJ, 295, 73

Kroupa, P., Tout, C. A., & Gilmore, G. 1993, MNRAS, 262, 545

Lanzetta, K. M., Fernández-Soto, A., & Yahil, A. 1998, in The Hubble Deep Field, ed. M. Livio, S. M. Fall & P. Madau, (Cambridge U. Press: Cambridge), in press

Lanzetta, K. M., Yahil, A., & Fernández-Soto, A. 1996, Nature, 381, 759

Leitherer, C., Ferguson, H. C., Heckman, T., & Lowenthal, J. 1995, ApJ, 454, L19

Lilly, S., et al. 1998, astro-ph/9712061

Lilly, S. J., Le Fevre, O., Crampton, D., Hammer, F., & Tresse, L. 1995a, ApJ, 455, 50

Lilly, S. J., Le Févre, O., Hammer, F., & Crampton, D. 1996, ApJ, 460, L1

Lilly, S. J., Tresse, L., Hammer, F., Crampton, D., & Le Fevre, O. 1995b, ApJ, 455, 108

Lin, H., Kirshner, R. P., Schectman, S. A., Landy, S. D., Oemler, A., Tucker, D. L., & Schechter, P. L. 1996, ApJ, 464, 60

Loveday, J., Peterson, B. A., Efstathiou, G., & Maddox, S. 1992, ApJ, 390, 338

Lowenthal, J. D., et al. 1996, ApJ, 481, 673

Madau, P. 1995, ApJ, 441, 18

Madau, P., Ferguson, H. C., Dickinson, M., Giavalisco, M., Steidel, C. C., & Fruchter, A. S. 1996, MNRAS, 283, 1388

Mann, R., et al. 1997, MNRAS, 289, 482

Massey, P., & Hunter, D. A. 1998, ApJ, 493, 180

McLeod, B. A., & Rieke, M. J. 1995, ApJ, 454, 611

Mendez, R. A., Minitti, D., Di Marchi, G., Baker, A., & Couch, W. J. 1996, MNRAS, 283, 666

Metcalfe, N., Shanks, T., Campos, A., Fong, R., & Gardner, J. P. 1996, Nature, 383, 236

Metcalfe, N., Shanks, T., Fong, R., & Roche, N. 1995, MNRAS, 273, 257

Meurer, G. 1998, in The Hubble Deep Field: Posters Presented at the STScI Symposium, Ma7 1997, ed. M. Livio, S. M. Fall & P. Madau, (Cambridge U. Press: Cambridge), in press

Miller, G. E., & Scalo, J. M. 1979, ApJS, 41, 513

Mo, H., & Fukugita, M. 1996, ApJ, 467, L9

Mobasher, B., Rowan-Robinson, M., Georgakakis, A., & Eaton, N. 1996, MNRAS, 282, L7

Mutz, S. B., et al. 1994, ApJ, 434, L55

Neuschaefer, L. W., & Windhorst, R. A. 1995, ApJ, 439, 14

Ogawa, T., Roukema, B. F., & Yamashita, K. 1997, ApJ, 484, 53

Oke, J. B. 1974, ApJS, 27, 21

Oliver, S. J., et al. 1997, MNRAS, 289, 471

Ortolani, S., Renzini, A., Gilmozzi, R., Marconi, G., Barbuy, B., Bica, E., & Rich, R. M. 1995, Nature, 377, 701

Padoan, P., Nordlund, A., & Jones, B. J. T. 1997, MNRAS, 288, 145P

Pei, Y. C., & Fall, S. M. 1995, ApJ, 454, 69

Persic, M., & Salucci, P. 1992, MNRAS, 258, 14P

Pettini, M., Steidel, C. C., Dickinson, M., Kellogg, M., Giavalisco, M., & Adelberger, K. L. 1997, in The Ultraviolet Universe at Low and High Redshift: Probing the Progress of Galaxy Evolution, ed. W. H. Waller, M. N. Fanelli, J. E. Hollis, & A. C. Danks

Phillips, A. C., Guzman, R., Gallego, J., Koo, D. C., Lowenthal, J. D., Vogt, N. P., Faber, S. M., & Illingworth, G. D. 1996, ApJ, 489, 543

Pozzetti, L., Bruzual, G., & Zamorani, G. 1996, MNRAS, 281, 953

Pozzetti, L., Madau, P., Zamorani, G., Ferguson, H., & Bruzual, G. 1998, astro-ph/9803144

Reid, I. N., Yan, L., Majewski, S., Thompson, I., & Smail, I. 1996, AJ, 112, 1472

Richards, E. A. 1998, in Observational Cosmology with the new Radio Surveys, ed. M. N. Bremer & a. et (Dordrecht: Kluwer), 273

Roche, N., Ratnatunga, K., Griffiths, R. E., Im, M., & Naim, A. 1998, MNRAS, 293, 157

Roche, N., Shanks, T., Metcalfe, N., & Fong, R. 1993, MNRAS, 263, 360

Roche, N., Shanks, T., Metcalfe, N., & Fong, R. 1996, MNRAS, 280, 397

Roukema, B. F., & Valls-Gabaud, D. 1997, ApJ, 488, 524

Rowan-Robinson, M., et al. 1997, MNRAS, 289, 490

Salpeter, E. E. 1955, ApJ, 121, 161

Sandage, A. 1961, ApJ, 133, 355

Sandage, A. 1988, ARA&A, 26, 561

Sawicki, M., & Yee, H. 1998, in The Hubble Deep Field: Posters Presented at the STScI Symposium, Ma7 1997, ed. M. Livio, S. M. Fall & P. Madau, (Cambridge U. Press: Cambridge), in press

Sawicki, M. J., Lin, H., & Yee, H. K. C. 1997, AJ, 113, 1

Schade, D., Lilly, S. J., Crampton, D., Hammer, F., Le Fevre, O., & Tresse, L. 1995, ApJ, 451, L1

Schechter, P. 1976, ApJ, 203, 297

Serjeant, S. B. G., et al. 1997, MNRAS, 289, 457

Skillman, E. D., Terlevich, R. J., Kennicutt, R. C., Garnett, D. R., & Terlevich, E. 1994, ApJ, 431, 172

Smail, I., Hogg, D. W., Yan, L., & Cohen, J. 1995, ApJ, 449, 105

Somerville, R. S., & Primack, J. R. 1998, astro-ph/9802268

Steidel, C., Dickinson, M., & Persson, E. 1994, ApJ, 437, L75

Steidel, C., Pettini, M., & Hamilton, D. 1996, AJ, 110, 2519

Steidel, C. C., Adelberger, K. L., Dickinson, M., Giavalisco, M., Pettini, M., & Kellog, M. A. 1998, ApJ, 492, 428

Steidel, C. C., Giavalisco, M., Dickinson, M., & Adelberger, K. L. 1996a, AJ, 112, 352

Steidel, C. C., Giavalisco, M., Pettini, M., Dickinson, M., & Adelberger, K. L. 1996b, ApJ, 462, 17

Tinsley, B. M. 1978, ApJ, 220, 816

Totani, T., Yoshii, Y., & Sato, K. 1997, ApJ, 483, L75

Tyson, J. A. 1988, AJ, 96, 1

Tytler, D., Fan, X. M., & Burles, S. 1996, Nature, 381, 207

van Dokuum, P., Franx, M., Kelson, D. D., Illingworth, G., Fisher, D., & Fabricant, D. 1998, astro-ph/9801190

Villumsen, J., Freudling, W., & da Costa, L. N. 1997, ApJ, 481, 578

Vogeley, M. 1997, astro-ph/9711209

Vogt, N. P., et al. 1997, ApJ, 479, L121

White, S. D. M., & Frenk, C. S. 1991, ApJ, 379, 52

White, S. D. M., & Rees, M. J. 1978, MNRAS, 183, 341

Wielen, R., Jahreiss, H., & Kruger, R. 1983, in IAU Colloq. 76, Nearby Stars and the Stellar Luminosity Function, ed. A. G. D. Phillip & A. R. Upgren (Schenectady: L. Davis), 163

Williams, R. E., et al. 1996, AJ, 112, 1335

Wilner, D., & Wright, M. C. H. 1997, ApJ, 488, L67

Windhorst, R. A., Fomalont, E. B., Kellerman, K. I., Partridge, R. B., Richards, E., Franklin, B. E., Pascarelle, S. M., & Griffiths, R. E. 1995, Nature, 375, 471

Yoshii, Y., & Peterson, B. 1994, ApJ, 436, 551

Yoshii, Y., & Peterson, B. A. 1995, ApJ, 444, 15

Yoshii, Y., & Takahara, F. 1988, ApJ, 326, 1

Zepf, S. 1997, Nature, 390, 377

Zepf, S. E., Moustakas, L. A., & Davis, M. 1997, ApJ, 474, L1